Circulators Using Planar Triangular Resonators

JOSEPH HELSZAJN, MEMBER, IEEE, DAVID S. JAMES, MEMBER, IEEE, AND W. TERENCE NISBET

Abstract—**This paper gives the theoretical description of 3-port circulators using planar triangular resonators. The standing-wave solution for this circulator is obtained by taking a linear combination of two $TM_{1,0,-1}$ standing waves with one of them rotated through 120°. The loaded Q factor for this junction is derived by forming the ratio of the energy stored in the circuit to that dissipated in the termination. The bandwidth of circulators using apex-coupled triangular resonators is three times that of circulators using conventional disk resonators. In the case of circulators using side-coupled triangular resonators, the bandwidth is one-third of that of the conventional arrangement.**

I. Introduction

STRIPLINE and waveguide junction circulators rely on either disk or triangular resonators for their operation. The theory of the waveguide circulator using triangular resonators has been treated by a number of authors [1]–[4], but no description of the stripline version is available although it has been used commercially for a number of years [5]. The purpose of this paper is to extend the Fay and Comstock treatment of the stripline circulator using a disk resonator [6] to that using a triangular one. The properties of planar triangular resonators have been described separately in [7]. One of its advantages is that its radiation Q factor is somewhat larger than that of a disk resonator. The theory of prism resonators has been treated in [8], [9].

Since the planar resonator may be either coupled midway along the sides of the triangle or at its corners, each situation is treated separately (Figs. 1(a) and (b)). However, a single standing-wave solution is found to apply to both arrangements. This standing-wave solution is obtained by taking a linear combination of two $TM_{1,0,-1}$ standing waves with one of them rotated through 120° with respect to the other. A field plot of the electric field distribution taken on an weakly coupled circulator confirms the adopted solution. The loaded Q factor for this junction is obtained by forming the ratio of the energy stored in the circuit to that dissipated in the termination. The bandwidth of the apex-coupled resonator is three times that of a single-disk one, while that coupled midway along the side of the triangle is one-ninth that of a disk resonator. The experimental and theoretical results are in good agreement for both geometries.

Manuscript received May 12, 1977; revised December 13, 1977. Some of the work described herein was undertaken at the Communication Research Centre, Department of Communications, Ott., Canada.

J. Helszajn and W. T. Nisbet are with the Department of Electrical Engineering, Heriot–Watt University, Edinburgh, Scotland, U.K.

D. S. James is with Solid-State Microwave Group, Ferranti Ltd., Manchester, England, U.K.

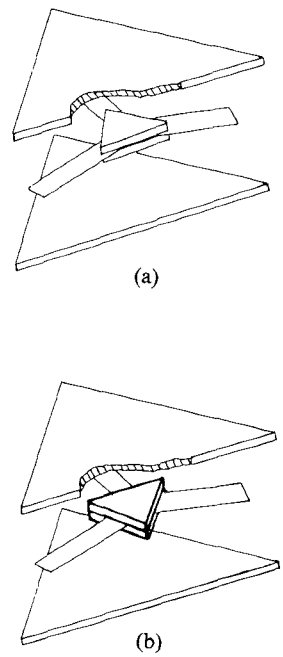

Fig. 1. Schematic diagrams of circulators using planar triangular resonators: (a) apex coupled, (b) sidewall coupled.

In formulating the boundary value problem of the apex-coupled triangular resonator, it is not necessary to partition it into an equivalent disk and tapered lines arrangement. Indeed, while it is difficult to visualize rotation of the field patterns in a planar triangular resonator, this is done directly.

II. TM Field Patterns of Triangular Open-Dielectric Resonator

The TM-mode field patterns in a triangular-shaped demagnetized ferrite or dielectric resonator with no variation of the field patterns along the thickness of the resonator are given by [7]

$$E_z = A_{m,n,l} T(x,y) \tag{1}$$

$$H_x = \frac{j}{\omega \mu_0 \mu_e} \frac{\delta E_z}{\delta y} \tag{2}$$

$$H_y = \frac{-j}{\omega \mu_0 \mu_e} \frac{\delta E_z}{\delta x} \tag{3}$$

and

$$H_z = E_x = E_y = 0 \tag{4}$$

0018-9480/79/0200-0188$00.75 ©1979 IEEE

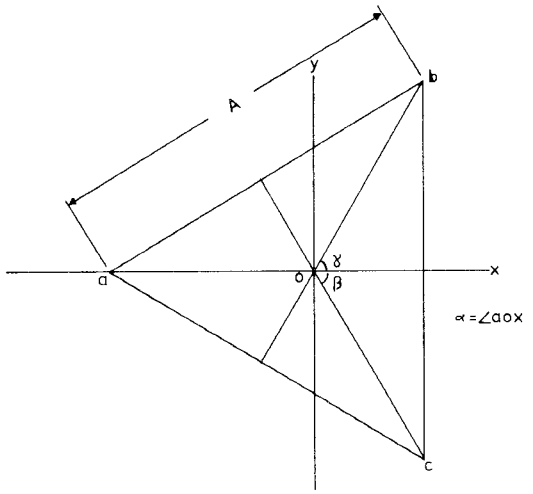

Fig. 2. Coordinate system of planar triangular resonator.

with $A_{m,n,l}$ an amplitude constant. Fig. 2 gives the schematic diagram of the planar resonator discussed in this text.

For magnetic boundary conditions, $T(x,y)$ may be obtained by duality from that of the TE mode with electric boundary conditions [10].

$$T(x,y)=\cos\frac{4\pi l}{\sqrt{3}\,A}\left(\frac{u}{2}+\frac{A}{2\sqrt{3}}\right)\cdot\cos\left[\frac{2\pi(m-n)(v-w)}{3\sqrt{3}\,A}\right]+\cos\frac{4\pi m}{\sqrt{3}\,A}\left(\frac{u}{2}+\frac{A}{2\sqrt{3}}\right)\cdot\cos\left[\frac{2\pi(n-l)(v-w)}{3\sqrt{3}\,A}\right]+\cos\frac{4\pi n}{\sqrt{3}\,A}\left(\frac{u}{2}+\frac{A}{2\sqrt{3}}\right)\cdot\cos\left[\frac{2\pi(l-m)(v-w)}{3\sqrt{3}\,A}\right] \quad (5)$$

where A is the side of the triangle, and

$$m+n+l=0 \quad (6)$$

which satisfies the wave equation

$$\left(\frac{\delta^2}{\delta x^2}+\frac{\delta^2}{\delta y^2}+k_{m,n,l}^2\right)E_z=0 \quad (7)$$

where

$$k_{m,n,l}=\frac{4\pi}{3A}\cdot\sqrt{m^2+mn+n^2}\ . \quad (8)$$

It is observed that the interchange of the three digits m,n,l leaves the cutoff number $k_{m,n,l}$ and field patterns unchanged.

The complete standing-wave solution for $m=1$, $n=0$, $l=-1$ is

$$E_z=A_{1,0,-1}T(x,y) \quad (9)$$

$$H_x=\frac{-jA_{1,0,-1}}{\omega\mu_0\mu_e}\left\{\frac{4\pi}{3A}\cos\left(\frac{2\pi u}{\sqrt{3}\,A}-\frac{2\pi}{3}\right)\sin\frac{2\pi(w-v)}{3\sqrt{3}\,A}+\frac{4\pi}{3A}\sin\frac{4\pi(w-v)}{3\sqrt{3}\,A}\right\} \quad (10)$$

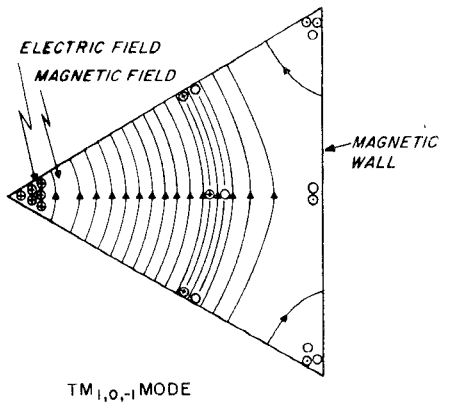

Fig. 3. $TM_{1,0,-1}$ field pattern in triangular resonator with magnetic walls.

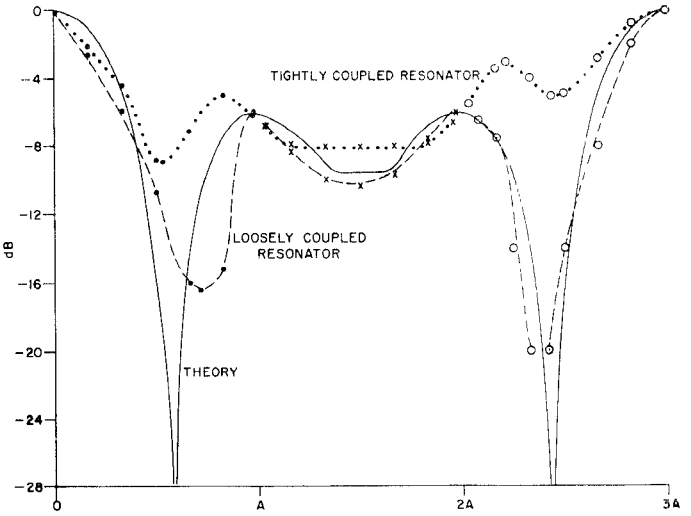

Fig. 4. Theoretical and experimental electric field distribution at edge of triangular resonator.

and

$$H_y=\frac{jA_{1,0,-1}}{\omega\mu_0\mu_e}\left\{\frac{4\pi}{3A}\sin\left(-\frac{2\pi u}{\sqrt{3}\,A}+\frac{2\pi}{3}\right)\cos\frac{2\pi(w-v)}{3\sqrt{A}}\right\}. \quad (11)$$

Fig. 3 gives the field patterns for the first mode in planar triangular resonators, while Fig. 4 gives the experimental electric field distribution for the $TM_{1,0,-1}$ mode, at the edge of the resonator for a microstrip device.

The resonant frequency of the dominant $TM_{1,0,-1}$ mode is given with the help of (8) by

$$kA=\frac{4\pi}{3}$$

with

$$k=\frac{2\pi}{\lambda_0}\sqrt{\epsilon_f\mu_e}$$

where ϵ_f is the relative dielectric constant of the ferrite material and μ_e is its relative permeability.

III. Electric Field Pattern in Circulators Using Triangular Resonator

The geometry of a triangular resonator makes it difficult to visualize rotation of the $TM_{1,0,-1}$ mode in order to satisfy the boundary conditions of an ideal circulator. However, one way it is possible to construct the electric field distribution is by taking a linear combination of two $TM_{1,0,-1}$ standing-wave solutions with one of them rotated through 120° with respect to the other. The standing-wave pattern for the dominant mode is

$$T(x,y)=2\cos\left(\frac{2\pi u}{\sqrt{3}\,A}+\frac{2\pi}{3}\right)\cos\left[\frac{2\pi(v-w)}{3\sqrt{3}\,A}\right]+\cos\left[\frac{4\pi(v-w)}{3\sqrt{3}\,A}\right]. \quad (12)$$

One field pattern is given with $\alpha=0$, $\beta=120°$, and $\gamma=240°$; this gives

$$u=x \quad (13)$$

$$v=-\frac{x}{2}+\frac{\sqrt{3}}{2}y \quad (14)$$

$$w=-\frac{x}{2}-\frac{\sqrt{3}}{2}y. \quad (15)$$

A second solution is obtained with $\alpha=120°$, $\beta=240°$, and $\gamma=360°$, giving

$$u=-\frac{x}{2}+\frac{\sqrt{3}}{2}y \quad (16)$$

$$v=-\frac{x}{2}-\frac{\sqrt{3}}{2}y \quad (17)$$

$$w=x. \quad (18)$$

The third field pattern is obtained with $\alpha=240°$, $\beta=360°$, and $\gamma=120°$ but is not necessary for the present discussion.

$$u=\frac{x}{2}-\frac{\sqrt{3}\,y}{2} \quad (19)$$

$$v=x \quad (20)$$

$$w=\frac{x}{2}+\frac{\sqrt{3}\,y}{2}. \quad (21)$$

The standing-wave solution for the circulator therefore, is, given by

$$T'(x,y)=T(x,y)^{0,\,120,\,240}-T(x,y)^{120,\,240,\,360} \quad (22)$$

where

$$T(x,y)^{0,\,120,\,240}=2\cos\left[\frac{2\pi x}{\sqrt{3}\,A}+\frac{2\pi}{3}\right]\cdot\cos\frac{2\pi y}{3A}+\cos\frac{4\pi y}{3A} \quad (23)$$

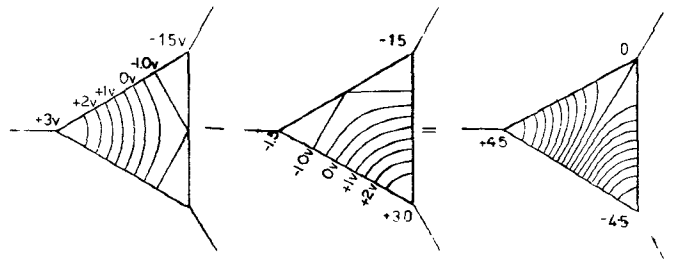

Fig. 5. Equipotential lines of circulator using apex-coupled planar triangular resonator in terms of linear combination of two $TM_{1,0,-1}$ standing-wave solutions with one of them rotated through 120°.

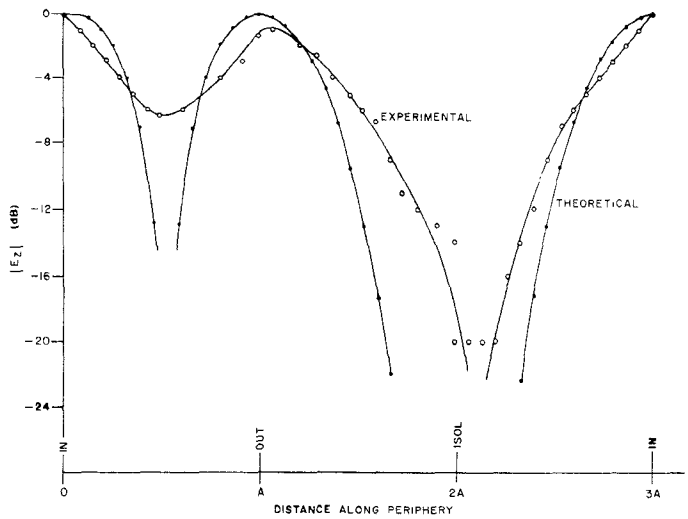

Fig. 6. Theoretical and experimental electric field distribution at edge of loosely coupled circulator using triangular resonator.

$$T(x,y)^{120,\,240,\,360}=2\cos\left[\frac{2\pi}{\sqrt{3}\,A}\left(-\frac{x}{2}+\frac{\sqrt{3}\,y}{2}\right)+\frac{2\pi}{3}\right]\cdot\cos\left[\frac{2\pi}{3\sqrt{3}\,A}\left(-\frac{3x}{2}+\frac{\sqrt{3}\,y}{2}\right)\right]+\cos\left[\frac{4\pi}{3\sqrt{3}\,A}\left(\frac{-3x}{2}+\frac{\sqrt{3}\,y}{2}\right)\right]. \quad (24)$$

Fig. 5 illustrates the construction of the standing-wave solution for the circulator using the equipotential diagram of the demagnetized resonator defined in [7].

Fig. 6 shows the theoretical and experimental electric field distribution at the edge of a loosely coupled circulator. The standing-wave solution defined by (22) can also be written as

$$T'(x,y)=T^{+}(x,y)e^{j30}+T^{-}(x,y)e^{-j30} \quad (25)$$

where

$$T'(x,y)^{\pm}=\frac{1}{3}\left[T(x,y)^{0,\,120,\,240}+T(x,y)^{120,\,240,\,360}\exp(\pm j120)+T(x,y)^{240,\,360,\,120}\exp(\pm j240)\right]. \quad (26)$$

The result for the $TM^{\pm}_{1,0,-1}$ mode is

$$T^{\pm}(x,y)_{1,0,-1}=\frac{1}{2}\exp\left(\mp j\frac{4\pi y}{3A}\right)+\cos\left(\frac{2\pi x}{\sqrt{3}\,A}+\frac{2\pi}{3}\right)\exp\left(\mp\frac{j2\pi y}{3A}\right). \tag{27}$$

It is easily verified that

$$T^{\pm}\left(\frac{-A}{\sqrt{3}},0\right)_{1,0,-1}=\frac{3}{2} \tag{28}$$

$$T^{\pm}\left(\frac{A}{2\sqrt{3}},\frac{A}{2}\right)_{1,0,-1}=\frac{3}{2}\exp(\mp j120) \tag{29}$$

$$T^{\pm}\left(\frac{A}{2\sqrt{3}},\frac{-A}{2}\right)_{1,0,-1}=\frac{3}{2}\exp(\mp j240). \tag{30}$$

The in-phase mode is given in a similar way in terms of $TM_{1,1,-2}$ as

$$T(x,y)_{1,1,-2}=\frac{1}{3}\left[T(x,y)^{0,120,240}+T(x,y)^{120,240,360}+T(x,y)^{240,360,120}\right]. \tag{31}$$

IV. Loaded Q Factor

The approach utilized here to obtain the loaded Q factor of the junction follows that employed by Fay and Comstock [6]. The loaded Q factor is defined by

$$Q_L=\frac{\omega U}{P_0} \tag{32}$$

where U is the stored energy in the two disks and P_0 is the power radiated out into the striplines. The stored energy is given by

$$U=2\cdot\iiint_v\frac{1}{2}\epsilon_0\epsilon_f\boldsymbol{E}^2\cdot dv. \tag{33}$$

E is the standing-wave solution given in (22) or (25) as

$$E=A_{1,0,-1}\left[T^{+}(x,y)e^{j\pi/6}+T^{-}(x,y)e^{-j\pi/6}\right]$$

and

$$T^{\pm}(x,y)=\frac{1}{2}\exp\left(\mp j\frac{4\pi y}{3A}\right)+\cos\left(\frac{2\pi x}{\sqrt{3}\,A}+\frac{2\pi}{3}\right)\cdot\exp\left(\pm j\frac{2\pi y}{3A}\right).$$

Evaluating (25) and substituting into (33) yields

$$U=\int_0^d\int_{-A/2\sqrt{3}}^{A/2\sqrt{3}}\int_{(-x/\sqrt{3})-(A/3)}^{(x/\sqrt{3})+(A/3)}\epsilon_0\epsilon_f A_{1,0,-1}\cdot\left[\cos\left(\frac{4\pi y}{3A}-\frac{\pi}{6}\right)+2\cos\left(\frac{2\pi x}{\sqrt{3}\,A}+\frac{2\pi}{3}\right)\cdot\cos\left(\frac{2\pi y}{3A}+\frac{\pi}{6}\right)\right]^2 dy\cdot dx\cdot dz$$

$$=0.64\epsilon_0\epsilon_f A_{1,0,-1}A^2\cdot d \tag{34}$$

where d is the thickness of each ferrite triangle. This result has been verified using a conversational numerals multiple-integration package available as a standard time-sharing utility on a Burrough's B5700 digital computer. The computed answer is

$$U=0.649\,519.$$

The total radiated power is given by

$$P_0=\frac{V^2}{R_0}=E_0^2\cdot d^2\cdot Y_0 \tag{35}$$

Y_0 is the conductance at the output stripline and also that looking into the resonator circuit, and E_0 is the electric field amplitude at the output port.

From (25) at $x=A/2\sqrt{3}$, $y=-A/2$

$$E_0=\frac{3\sqrt{3}}{2}A_{1,0,-1}. \tag{36}$$

Thus P_0 becomes

$$P_0=\frac{27}{4}A^2_{1,0,-1}\cdot d^2Y_0. \tag{37}$$

Forming Q_L yields

$$Q_L=\frac{0.095\epsilon_0\epsilon_f\omega A^2}{Y_0 d}. \tag{38}$$

This may be compared with the value for a simple disk given by Fay and Comstock.

$$Q_L=\frac{1.48\epsilon_0\epsilon_f\omega R^2}{Y_0 d}. \tag{39}$$

Forming the ratio of the loaded Q factors given above yields

$$\frac{Q_L(\Delta)}{Q_L(0)}=0.332 \tag{40}$$

indicating that the bandwidth for triangular resonators is three times that for disk resonators.

V. Circulators Using Triangular Resonators Coupled Midway Along Its Side Walls

The symmetry of triangular resonators indicates that an alternative circulator solution to that of the apex-coupled junction is one where the input transmission lines are coupled midway along the side wall of the triangle. Inspection of Fig. 7 indicates that a combination of $TM_{1,0,-1}$ modes also satisfies this coupling arrangement. Since this solution relies on the same field patterns as the apex-coupled one, the operating frequency is that given by (8).

The evaluation of the Q factor for this geometry proceeds as in the previous section. Since the field patterns are identical to those of the apex-coupled arrangement, the stored energy will be that previously evaluated in (34). The electric field at one output port, i.e., at $(A/2\sqrt{3}, 0)$

will be modified from (36) to

$$E_0 = \frac{\sqrt{3}}{2} A_{1,0,-1}. \tag{41}$$

Forming the loaded Q as in the previous section yields

$$Q_L = \frac{0.855 \cdot \epsilon_0 \epsilon_f \omega A^2}{Y_0 d}. \tag{42}$$

The Q factor of this geometry is therefore 9 times that of the apex-coupled circulator and 3 times that of the conventional disk arrangement.

VI. Bandwidth and Gyrator Admittance

Once the loaded Q factor is given, the bandwidth is defined by

$$Q_L \approx \frac{r-1}{\sqrt{r}\, 2\delta_0} \tag{43}$$

where

$$2\delta_0 = \frac{\omega_2 - \omega_1}{\omega_0} \tag{44}$$

r is the VSWR, $\omega_{1,2}$ are the band edges, and ω_0 is the center frequency.

It is also possible to make a statement about the gyrator level [11] of the circulator by invoking the universal relation between the loaded Q factor and the split frequencies $\omega_\pm$ of the magnetized junction.

$$\frac{1}{Q_L} = \sqrt{3}\left(\frac{\omega_+ - \omega_-}{\omega_0}\right). \tag{45}$$

This relation can also be written as

$$Y_0 = \sqrt{3}\, B'\left(\frac{\omega_+ - \omega_-}{\omega_0}\right) \tag{46}$$

by noting that

$$Q_L = \frac{B'}{Y_0} \tag{47}$$

where B' is the susceptance slope parameter of the junction, and Y_0 is the characteristic admittance of the transmission lines

$$Y_0 = \left\{30\pi \ln\left[\frac{W+b}{W+t}\right]\right\}^{-1}. \tag{48}$$

This last equation allows W to be calculated once b is set by the loaded Q factor.

The approximate form for the split frequencies $\omega_\pm$ based on circular variables often used in the case of disk resonators (in terms of the elements of the tensor permeability) will be adopted here also.

$$\frac{\omega_+ - \omega_-}{\omega_0} \simeq 0.7\frac{K}{\mu}. \tag{49}$$

This assumption has been verified by measuring the split frequencies of both types of resonators [11]. The result is given in Fig. 8.

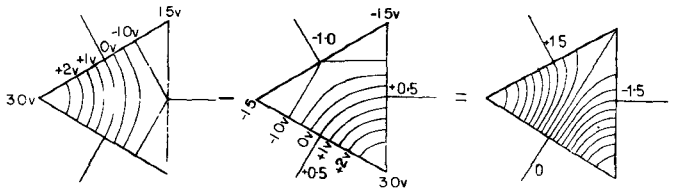

Fig. 7. Equipotential lines of circulator using sidewall-coupled planar triangular resonator in terms of linear combination of two $TM_{1,0,-1}$ standing-wave solutions with one of them rotated through 120°.

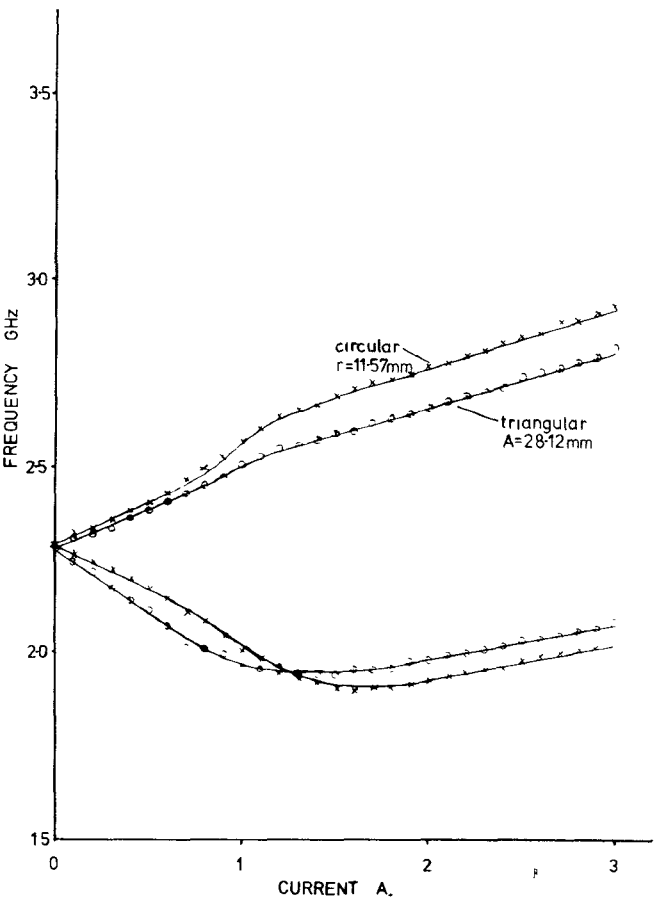

Fig. 8. Experimental split frequencies for disk- and apex-coupled triangular resonators.

VII. Experimental and Theoretical Q Factors for Disk and Triangular Resonators

The Q factor of junction circulators may be evaluated from their frequency characteristics in conjunction with (43). A number of circulators with different ground plane spacings were therefore constructed using disk-, side-, and apex-coupled triangular resonators. The material used in these circulators had a magnetization of 0.0400 Wb/m^2 and a dielectric constant of $\epsilon_f = 15.3$. The construction of the circulators using the triangular resonators are depicted in Fig. 1.

In the case of the triangular resonator, the A dimension was held constant at 28 mm and the thickness was varied between 1.27 and 3.175 mm. The center frequency for this device was approximately 2.256 GHz. In the case of the

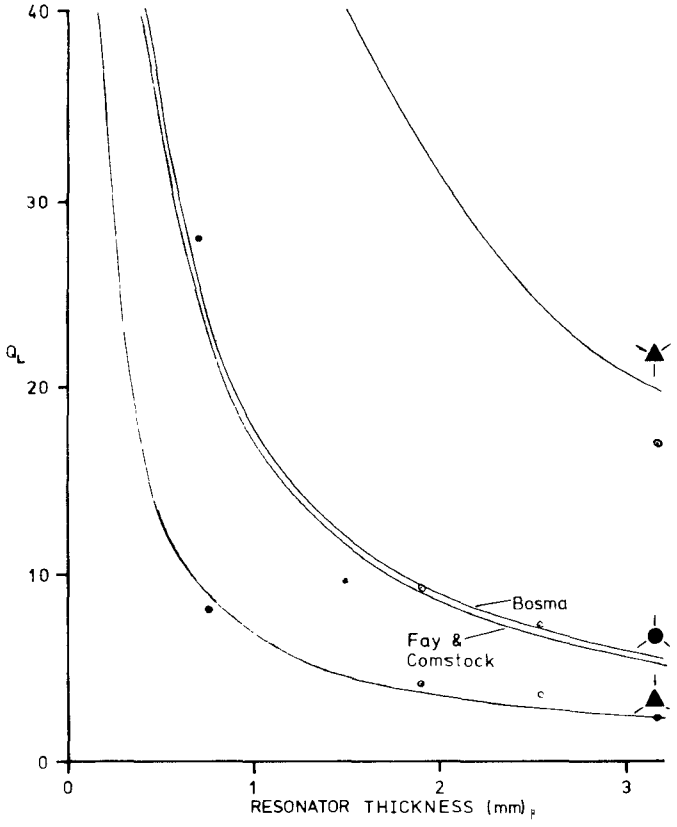

Fig. 9. Experimental and theoretical Q factors for circulators using disk and triangular planar resonators.

disk resonator, the radius was held constant at 9.9 mm and its thickness was varied in the same range. The center frequency for this arrangement was 2.8 GHz.

Fig. 9 summarizes the theoretical values of the Q factor obtained using (38) and (39) with the experimental ones obtained by measuring the 20-dB bandwidth of the circulators in conjunction with (43). In the case of the disk resonator, the Bosma expression for the Q factor is also plotted [12]. Good agreement between theory and experiment is found for all geometries showing that the theoretical loaded Q factor for disk and triangular resonators may be calculated with reasonable accuracy.

Due to the relatively large values of loaded Q factor associated with the side-coupled resonators, it was not possible to obtain a reliable measurement of this parameter except in the 3.175-mm thick case.

VIII. Conclusions

This paper has developed the theory of planar circulators using triangular instead of disk resonators to establish the junction resonance. The experimental and theoretical results indicate that the bandwidth of circulators using apex-coupled resonators is three times that of the more conventional devices using disk resonators, while the bandwidth of junction circulators using side-coupled resonators is a third that of conventional junctions.

References

[1] J. G. Leetma, "Ferrite circulator with conductive plate of uniform thickness having tapered angular apexes for broad banding," U.S. Patent no. 3 104 361, Sept. 17, 1963.

[2] F. M. Aitken and R. McLean, "Some properties of the waveguide *Y* circulator," *Proc. Inst. Elec. Eng.*, vol. 110, no. 2, Feb. 1963.

[3] Y. Akaiwa, "Operation modes of a waveguide *Y*-circulator," *IEEE Trans. Microwave Theory Tech.*, vol. MTT-22, pp. 954–959, Nov. 1974.

[4] Y. Akaiwa, "Mode classification of a triangular ferrite post for *Y*-circulator," *IEEE Trans. Microwave Theory Tech.*, vol. MTT-25, pp. 59–61, Jan. 1977.

[5] Western Microwave, California, private communication.

[6] C. E. Fay and R. L. Comstock, "Operation of the ferrite junction circulator," *IEEE Trans. Microwave Theory Tech.*, vol. MTT-13, pp. 15–27, Jan. 1965.

[7] J. Helszajn and D. S. James, "Planar triangular resonators with magnetic walls," *IEEE Trans. Microwave Theory Tech.*, vol. MTT-26, pp. 95–100, Feb. 1978.

[8] A. G. Medoks, "Design of a waveguide *Y*-circulator," *Telecommun. Radio Eng.*, vol. 22, pt. 2, no. 9, Sept. 1967.

[9] N. Ogasawara and T. Noguchi, "Model analysis of dielectric resonator of the normal triangular cross-section," presented at the 1974 Ann. Nat. Conv. Inst. Elec. Eng., Japan, Mar. 28, 1974.

[10] Schelkunoff, *Electromagnetic Waves*. New York: Van Nostrand, 1943, p. 393.

[11] J. Helszajn, *Non-Reciprocal Microwave Junctions and Microwave Circulators*. New York: Wiley Interscience, 1975.

[12] H. Bosma, "On stripline circulation at UHF," *IEEE Trans. Microwave Theory Tech.*, vol. MTT-12, pp. 61–72, Jan. 1964.